Int. J. Heat Mass Transfer. Vol. 28, No. 10, pp. 1805–1812, 1985
Printed in Great Britain

0017–9310/85 $3.00 + 0.00

On a heat transport model for a turbulent plane jet

R. A. ANTONIA
Department of Mechanical Engineering, University of Newcastle, N.S.W., 2308, Australia

(*Received* 12 *March* 1984 *and in final form* 23 *October* 1984)

Abstract—Distributions of the temperature–pressure gradient correlations are obtained from measured budgets of the longitudinal and lateral heat fluxes in the self-preserving region of a slightly heated turbulent plane jet into still air. These correlations are consistent with a model which includes only the turbulence interaction contribution to the pressure fluctuations. The comparison between model and experiment is not affected by the choice of time scale in the model. Terms whose gradients form the major contribution to diffusion in the budgets for heat fluxes and the temperature variance are only qualitatively consistent with gradient-type models.

INTRODUCTION

IN THE LAST few years, increased attention (e.g. refs. [1–5]) has been given to second-order models for scalar transport in laboratory turbulent shear flows. Although the models should in general be able to deal with variations in fluid properties, most of the models have concentrated on flows where the scalar is passive and does not therefore influence the dynamics of the flow. Second-order models can be tackled at various levels of complexity. A scheme that is gaining in popularity includes transport equations for the heat fluxes, the temperature variance and the dissipation or destruction of the temperature variance (e.g. refs. [1, 4, 6, 7, 8]).

In this paper models for several terms in approximations for transport equations of $\overline{u\theta}$, $\overline{v\theta}$ and $\overline{\theta^2}$ are compared with measurements obtained in a slightly heated plane jet into still air. The primary emphasis is on the experimental budgets of the longitudinal and lateral heat fluxes and on the pressure–temperature gradient correlations derived by difference from these budgets. Experimental budgets for the same flow of $\overline{\theta^2}$ and $\overline{(\partial\theta/\partial x)^2}$ were published earlier [9, 10]. The budget of $\overline{\theta^2}$ [9] demonstrated that satisfactory closure could be obtained provided that all components of the destruction N were included. The measured budget of N is not yet within your grasp and models for terms in the transport equations for N have been proposed without the benefit of experiment.

TRANSPORT EQUATIONS FOR THE SCALAR FIELD

Equations for the heat flux vector, the temperature variance $\overline{\theta^2}$ and the square of the temperature gradient (proportional to the temperature destruction) were written by Corrsin [11]. It is sufficient here to write approximations, relevant to the present flow, to these coupled equations.

The transport equation for the longitudinal heat flux $\overline{u\theta}$ is given by

$$\underbrace{\bar{U}\frac{\partial}{\partial x}(\overline{\theta u})+\bar{V}\frac{\partial}{\partial y}(\overline{\theta u})}_{\text{I}}+\underbrace{\overline{u^2}\frac{\partial\bar{T}}{\partial x}+\overline{u\theta}\frac{\partial\bar{U}}{\partial x}+\overline{uv}\frac{\partial\bar{T}}{\partial y}+\overline{v\theta}\frac{\partial\bar{U}}{\partial y}}_{\text{II}}+\underbrace{\frac{\partial}{\partial y}(\overline{uv\theta})}_{\text{III}}+\underbrace{\theta\overline{\frac{\partial p}{\partial x}}}_{\text{IV}}=0 \quad (1)$$

where I, II, III, IV can be interpreted as the advection, production, diffusion and destruction terms respectively (the Roman numerals retain this interpretation in equations that follow).

Transport equations for the lateral heat flux $\overline{v\theta}$ and for $\overline{\theta^2}/2$ are approximated by

$$\underbrace{\bar{U}\frac{\partial}{\partial x}(\overline{\theta v})+\bar{V}\frac{\partial}{\partial y}(\overline{\theta v})}_{\text{I}}+\underbrace{\overline{v^2}\frac{\partial\bar{T}}{\partial y}}_{\text{II}}+\underbrace{\frac{\partial}{\partial y}(\overline{v^2\theta})}_{\text{III}}+\underbrace{\theta\overline{\frac{\partial p}{\partial y}}}_{\text{IV}}=0 \quad (2)$$

and

$$\underbrace{\bar{U}\frac{\partial}{\partial x}\left(\frac{\overline{\theta^2}}{2}\right)+\bar{V}\frac{\partial}{\partial y}\left(\frac{\overline{\theta^2}}{2}\right)}_{\text{I}}+\underbrace{\overline{v\theta}\frac{\partial\bar{T}}{\partial y}+\overline{u\theta}\frac{\partial\bar{T}}{\partial x}}_{\text{II}}+\underbrace{\frac{\partial}{\partial y}\left(\frac{\overline{v\theta^2}}{2}\right)}_{\text{III}}+\underbrace{N}_{\text{IV}}=0. \quad (3)$$

The transport equation for N, the destruction of $\overline{\theta^2}/2$, was considered by Corrsin [11] and others (e.g. [12, 13]). As discussed in [10], the majority of the terms in this equation are not readily amenable to experimental verification. Although the majority of the terms in the transport equation for $\overline{(\partial\theta/\partial x)^2}$ have been

NOMENCLATURE

a_1 stress intensity ratio, $\overline{uv}/\overline{q^2}$
a_θ structure parameter for the thermal field, $\overline{v\theta}/(\overline{\theta^2}^{1/2}\overline{uv}^{1/2})$
c, d constants in equation (6)
$c_{1\theta}$ constant in equation (5)
d nozzle width [m]
L_u half-maximum velocity width [m]
N average dissipation of $\overline{\theta^2}/2$, defined as $\alpha[\overline{(\partial\theta/\partial x)^2}+\overline{(\partial\theta/\partial y)^2}+\overline{(\partial\theta/\partial z)^2}]$, [°C^2 s^{-1}]
p kinematic pressure fluctuation [m^2 s^{-2}]
Pr_t turbulent Prandtl number, $\overline{uv}(\partial\bar{T}/\partial y)\sqrt{v\theta}(\partial\bar{U}/\partial y)$
$\overline{q^2}$ total turbulent intensity, $\overline{u^2}+\overline{v^2}+\overline{w^2}$ [m^2 s^{-2}]
R ratio of dynamic and scalar time scales, τ_θ/τ_u
$\bar{T}$ mean temperature relative to ambient [°C]
u, v, w velocity fluctuations in x-, y- and z-directions [m s^{-1}]
$\overline{uv}$ average kinematic Reynolds shear stress [m^2 s^{-2}]
$\overline{u\theta}$ average thermometric longitudinal heat flux [m s^{-1} °C^{-1}]
$\bar{U}, \bar{V}$ mean velocities in x- and y-directions [m s^{-1}]
$\overline{v\theta}$ average thermometric lateral heat flux [m s^{-1} °C^{-1}]
x longitudinal or streamwise direction, with origin at nozzle [m]
y in direction of main shear, with origin at centre line [m]
z spanwise direction [m].

Greek symbols
α molecular thermal diffusivity [m^2 s^{-1}]
ε average dissipation of $\overline{q^2}/2$ [m^2 s^{-3}]
η non-dimensional distance y/L_u
θ temperature fluctuation [°C]
$\overline{\theta^2}$ temperature variance [°C^2]
ν kinematic viscosity [m^2 s^{-1}]
τ_u time scale for dynamic field, $\overline{q^2}/2\varepsilon$ [s]
τ_u' $\tau_u/c_{1\theta}$
τ_θ time scale for thermal field, $\overline{\theta^2}/2N$ [s].

Subscripts and other symbols
j refers to conditions at nozzle exit
0 refers to conditions at centreline
$\bar{}$ denotes conventional time average.

determined experimentally [10], it is premature to use these results for modelling the equation for N. Models that have been proposed for this equation will not be considered here.

Stationarity of the flow and order of magnitude arguments, based on the boundary-layer approximation and sufficiently large values of the Reynolds and Péclet numbers, were used to neglect terms that do not appear in equations (1)–(3). These transport equations together with the transport equation for N and that for the mean temperature

$$\bar{U}\frac{\partial\bar{T}}{\partial x}+\bar{V}\frac{\partial\bar{T}}{\partial y}+\frac{\partial}{\partial x}(\overline{u\theta})+\frac{\partial}{\partial y}(\overline{v\theta})\simeq 0 \qquad (4)$$

provide a reasonably complete description of the scalar field, once the velocity field is calculated.

EXPERIMENTAL DETAILS

A detailed account of the experimental arrangement is given in [9]. Since hot wire/cold wire techniques required for the measurement of terms in equations (1)–(3) have been described in [9], only a brief summary of the experimental arrangement is given here with emphasis on experimental conditions.

The plane jet issues from a nozzle of width d = 12.7 mm and height 250 mm. Two confining horizontal plates (width $\simeq$ 700 mm, length $\simeq$ 1100 mm) are located at the top and bottom of the nozzle to help maintain the two-dimensionality of the flow. The jet is heated to a temperature of about 25°C above ambient. A nominal jet velocity of 9 m s^{-1}, at the nozzle exit, was used which corresponded to a Reynolds number, based on d, of about 7600. The boundary layers are laminar at the nozzle exit with velocity distributions in close agreement with the Blasius profile.

Approximate self-preservation of the far field jet flow was established at $x/d \simeq 20$ on the basis of different types of measurement. These included distributions of mean velocity, mean temperature, Reynolds stresses, the temperature variance, heat fluxes and high-order moments of velocity and temperature fluctuations. All the results presented in this paper were obtained from measurements at $x/d = 40$. At this location, U_0, the mean velocity at the centreline, is 3.4 m s^{-1} while T_0, the corresponding mean temperature, is about 9°C above ambient and the mean velocity half-width L_u is 60 mm. Streamwise variations of U_0, T_0 and L_u have been reported in [9].

As noted in [9], flow reversal was first detected at a value of η ($\equiv y/L_u$) of about 1. At this location, the intensity and frequency of flow reversal are small but at larger values of η, there is an increase in both these parameters with a deterioration in the accuracy of measurement. Goldschmidt *et al.* [14] indicated that no flow reversal occurred (in a plane jet into still air) for

$\eta \lesssim 1.6$, on the basis of a thermal wake detection experiment similar to that used in [9]. The wake detection results of [14] do not completely rule out the possibility of flow reversal but with a small (<4%) probability of occurrence at smaller values of η. The temperature variance $\overline{\theta^2}$ was measured with a single cold wire placed immediately upstream of an × -wire and with the same cold wire without the × -wire. The first measurement deviated from the second only when $\eta \gtrsim 1.2$, suggesting that the temperature statistics are unlikely to be affected by flow reversal in the range $0 < \eta < 1$. The × -wire measurements may be in error in this range due to the velocity vector being occasionally inclined at angles greater than 45°. A reliable estimate of this error would require independent measurements with either laser or pulsed wire anomometers. Measurements of terms in equation (3) were obtained for lateral distances extending to $\eta \simeq 1.3$; accordingly, terms in equations (1) and (2) are shown up to $\eta \simeq 1.3$.

BUDGETS OF HEAT FLUXES AND COMPARISON WITH MODELS

Terms in equations (1) and (2) have been normalised by multiplying by $L_u/U_0^2T_0$ and are plotted in Figs. 1 and 2 respectively. Also shown in these figures are measured distributions of $\overline{u\theta}$ and $\overline{v\theta}$. Evaluation of the terms in equations (1) and (2) was carried out using the experimentally verified assumption of self-preservation. Cubic spline least-square fits to experimental data for $\bar{U}/U_0$, $\bar{T}/T_0$, $\overline{\theta^2}/T_0^2$, $\overline{uv}/U_0^2$, $\overline{u\theta}/U_0T_0$, $\overline{v\theta}/U_0T_0$, $NL_u/U_0T_0^2$ were implemented on a digital computer. Derivatives with respect to η were determined by numerical differentiation; least-square fits were applied to the estimates for the derivatives. Terms involving derivatives with respect to x were rewritten using self-preservation so as to involve derivatives with respect to η and the known variation with respect to x of quantities such as L_u, U_0 and T_0. The lateral mean velocity $\bar{V}$ was calculated from the continuity equation. Before discussing the $\overline{u\theta}$ and $\overline{v\theta}$ budgets, it is pertinent to note that the measured distributions of $\overline{v\theta}$ and $\overline{uv}$ were found [15] to be in reasonable agreement with calculations of these quantities via the mean enthalpy equation (4) and the mean momentum equations. The largest deviation between calculation and measurement was of the order of 13%, at $\eta \simeq 0.7$.

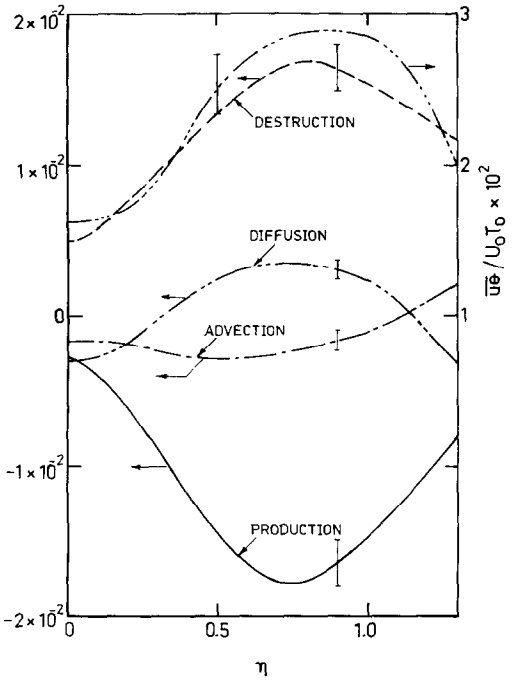

FIG. 1. Longitudinal heat flux budget. Terms in equation (1) are multiplied by $L_u/U_0^2T_0$. ——, advection I; —, production, II; — · — · —, diffusion III; — —, destruction IV; — · — · —, $u\theta/U_0T_0$. (Error bars in this and subsequent figures indicate estimated rms errors.

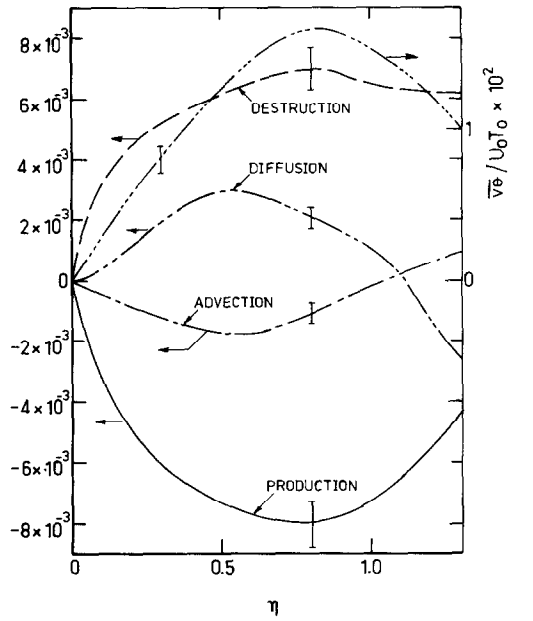

FIG. 2. Lateral heat flux budget. Terms in equation (2) are multiplied by $L_u/U_0^2T_0$. — · — · —, $v\theta/U_0T_0$. Other symbols are as in Fig. 1.

The diffusion and advection terms in the $\overline{u\theta}$ budget (Fig. 1) have the same sign near the centreline, qualitatively reflecting the behaviour of advection and diffusion terms in the budget for $\overline{\theta^2}/2$ [9]. At the centreline, the destruction, determined by difference, is almost twice as large as the production. Away from the centreline ($\eta \gtrsim 0.4$), the diffusion and advection terms are of opposite sign and approximately equal magnitude. It follows that the production and destruction terms are approximately in balance in this region of the flow, reaching maxima near $\eta = 0.8$. Although the diffusion term $\partial(\overline{uv\theta})/\partial y$ is significantly larger than $\partial(\overline{u^2\theta})/\partial x$ [not included in term III of equation (1)] near the centreline, the production terms $-\overline{u^2}\,\partial\bar{T}/\partial x$ and $-\overline{u\theta}\,\partial\bar{U}/\partial x$ are important there

($\eta \lesssim 0.4$) and were consequently retained in equation (1). For $\eta \gtrsim 0.4$, the terms $-\overline{uv}\,\partial\bar{T}/\partial y$ and $-\overline{v\theta}\,\partial\bar{U}/\partial y$ provide the major contribution to production. The contribution of $-\overline{u\theta}\,\partial\bar{T}/\partial x$ to the $\overline{\theta^2}$ budget, equation (3), is only important near the centreline and was not included in [9].

Advection and diffusion terms of the $\overline{v\theta}$ budget (Fig. 2) are opposite in sign and approximately equal in magnitude across the jet. Consequently, production and destruction are in balance everywhere and not simply in the region $\eta \gtrsim 0.4$, as in the $\overline{u\theta}$ budget. The other major difference between Figs. 1 and 2 is the larger importance, in Fig. 2, of advection and diffusion terms relative to the production and destruction terms.

The magnitude of the pressure–temperature gradient correlations in Figs. 1 and 2 corroborates previous experimental evidence, in both laboratory (e.g. [16]) and atmospheric flows (e.g. [17, 18]), for the importance of these correlations. General models for the pressure–temperature gradient correlations have included contributions due to turbulence, the mean rate of strain and the gravitational field (e.g. [13]). The simplest model, which includes only the first contributions, can be written

$$\overline{p\frac{\partial\theta}{\partial x}} = -c_{1\theta}\left(\frac{2\varepsilon}{\overline{q^2}}\right)\overline{u\theta} \tag{5a}$$

or

$$\overline{p\frac{\partial\theta}{\partial y}} = -c_{1\theta}\left(\frac{2\varepsilon}{\overline{q^2}}\right)\overline{v\theta} \tag{5b}$$

where the ratio $\overline{q^2}/2\varepsilon$ can be identified as the turbulence relaxation time τ_u or lifetime for the energy containing eddies. The time scale τ_u in equations (5a and b) was interpreted as the ratio of a length scale and a velocity scale (e.g. $\overline{q^2}^{1/2}$) in earlier proposals (e.g. Monin [19]; Donaldson *et al.* [20]) for the pressure–temperature gradient correlation. Launder [13] notes that it is likely that the time scale in equations (5) should preferably contain some weighting from the time scale τ_θ ($\equiv \overline{\theta^2}/2N$) of the thermal field. This should be unnecessary in near-equilibrium conditions for which τ_θ is expected to be proportional to τ_u. The ratio R ($=\tau_\theta/\tau_u$) for the present flow increases slightly (Fig. 3) in the region $0.4 \leqslant \eta \leqslant 1.3$ where budgets of $\overline{u\theta}$ and $\overline{v\theta}$ exhibit approximate equality between production and destruction. The magnitude of R is closer, however, to unity than to about 0.5, the value obtained by Béguier *et al.* [21] in several near-equilibrium flows. This difference will be discussed in the following section.

With the assumption that $\overline{p\,\partial\theta/\partial x} \simeq -\overline{\theta\,\partial p/\partial x}$,* $c_{1\theta}$ was estimated (Fig. 4) from the distributions of the destruction term (Fig. 1) and of τ_u (Fig. 3). In the region

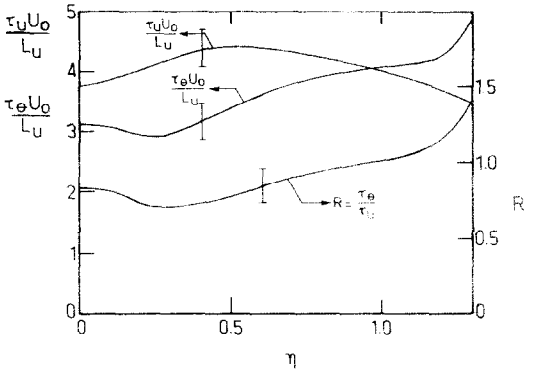

FIG. 3. Time scales of the dynamic and scalar fields and their ratio.

$0.4 \leqslant \eta \leqslant 1.3$, $c_{1\theta}$ lies in the range 2–2.5 with an average value of 2.26 (± 0.06). The testing of equation (5b) against experimental distributions resulted in values of $c_{1\theta}$ in the range 1.7–2.3 with an average of about 1.94 (± 0.06). The agreement between these two estimates of $c_{1\theta}$ seems satisfactory given the uncertainty of about $\pm 10\%$ in the LHSs of equations (5a and b). This agreement is not surprising since, although the ratio $\overline{u\theta}/\overline{v\theta}$ is nearly 2 (Fig. 4), $\overline{p\,\partial\theta/\partial x}$ (Fig. 1) is nearly twice as large as $\overline{p\,\partial\theta/\partial y}$ (Fig. 2). The use of τ_θ or a hybrid time scale $(\tau_\theta\tau_u)^{1/2}$ instead of τ_u in equation (5a) does not significantly affect the magnitude of $c_{1\theta}$ (Fig. 5). The average value of $c_{1\theta}$ in the range $0.4 \leqslant \eta \leqslant 1.3$ is equal to 2.19 when τ_θ is used and 2.21 when $(\tau_\theta\tau_u)^{1/2}$ is chosen.

Another form of the pressure–temperature gradient correlation considered by Launder [13] can be written

$$\overline{p\frac{\partial\theta}{\partial x}} = -c\frac{\overline{u\theta}}{\tau_u} - d\frac{\overline{v\theta}}{\tau_u} \tag{6}$$

where $c = c_{1\theta} + 2c'_{1\theta}(\overline{u^2}/\overline{q^2} - 1/2)$ and $d = 2a_1c'_{1\theta}$, with $a_1 = \overline{uv}/\overline{q^2}$. This formulation is not expected to differ appreciably from equations (5) in the region of interest since the ratio $\overline{u\theta}/\overline{v\theta}$ is approximately constant (Fig. 4). A least-squares regression to the experimental data for $\overline{\theta\,\partial p/\partial x}$, $\overline{u\theta}$, $\overline{v\theta}$ and τ_u yielded values of $c_{1\theta}$ and $c'_{1\theta}$ equal to 2.63 and -1.15, respectively. Elghobashi and

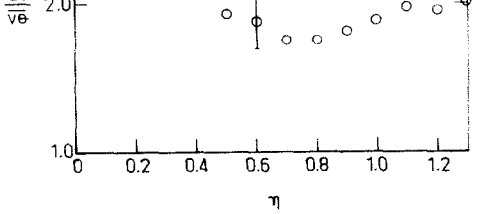

FIG. 4. Ratio of longitudinal and lateral heat fluxes.

*An order of magnitude argument shows that $\partial(\overline{p\theta})/\partial x$ is smaller than either $\overline{p\,\partial\theta/\partial x}$ or $-\overline{\theta\,\partial p/\partial x}$ by a ratio L/λ where L and λ are turbulence integral and Taylor microscales, respectively. This ratio should be of order 10 for the present Reynolds number.

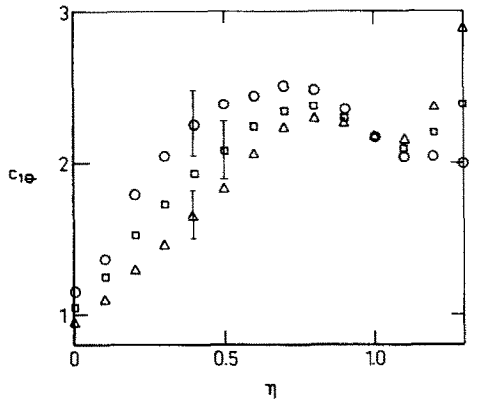

FIG. 5. Distributions of $c_{1\theta}$ for different choices of the time scale. ○, τ_u; △, τ_θ; □, $(\tau_u\tau_\theta)^{1/2}$.

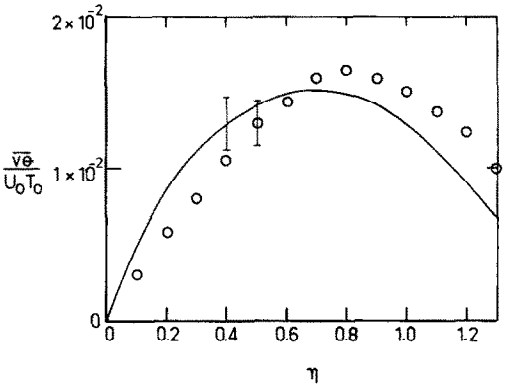

FIG. 6. Comparison of measured lateral heat flux distribution with equation (7). ○, experiment; ——, equation (7), $c_{1\theta} = 2.26$.

Launder [7] quote values of 2.15 and -1.6 for $c_{1\theta}$ and $c'_{1\theta}$ associated with τ_θ. Launder [13] already noted that available values of $c_{1\theta}$ are not significantly affected by the inclusion of the mean rate of strain in the model for $\overline{p\,\partial\theta/\partial x}$. This result is supported by the present data since the addition of a strain rate term to the RHS of equation (6), of the form $0.5\,[\overline{v\theta}\,\partial\bar{U}/\partial y + \overline{u\theta}\,\partial\bar{U}/\partial x]$, resulted in only a 16% decrease in the magnitudes of both $c_{1\theta}$ and $c'_{1\theta}$.

The present magnitude of $c_{1\theta}$, regardless of whether equations (5) or (6) are used, is significantly different from values of about 4.3 inferred, using equation (5a), from the measurements of Antonia and Danh [22] in the outer part of a boundary layer and about 4.8 for a round jet with a co-flowing stream (Antonia and Prabhu [16]. Recently, Jones and Musonge [4] used a value of 1.0 for $c_{1\theta}$, estimated from free shear flow data. Launder [13] has already referred to the large variation in $c_{1\theta}$. All available estimates of $c_{1\theta}$ appear to indicate that a universal value does not exist.

The magnitude of $c_{1\theta}$, as obtained from equation (5a), can be tested by comparing the following two expressions (Launder [13])

$$\overline{v\theta} = -c_{1\theta}^{-1}\tau_u\overline{v^2}\frac{\partial\bar{T}}{\partial y} \tag{7}$$

$$Pr_t = 2c_{1\theta}a_1^2\frac{\overline{q^2}}{\overline{v^2}} \tag{8}$$

with measured distributions of the lateral heat flux $\overline{v\theta}$ and the turbulent Prandtl number Pr_t. Equation (7) assumes equality between production (II) and dissipation (IV) terms in the $\overline{v\theta}$ equation (2). Equation (8) further requires a balance between production and dissipation of $\overline{q^2}$. The comparison, with $c_{1\theta} = 2.26$, seems satisfactory in the case of $\overline{v\theta}$ (Fig. 6). It is also adequate in the case of Pr_t (Fig. 7) in the region where assumptions for (7) and (8) are approximately satisfied. The comparison breaks down near $\eta = 0$ since these assumptions are violated in this region.

Triple products whose gradients are interpreted as the diffusion terms in transport equations for the heat fluxes and the temperature variances are often modelled using a gradient–diffusion assumption. The models can be written (ignoring gradients with respect to x)

$$\overline{uv\theta} = -\tau'_u\left(\overline{uv}\frac{\partial}{\partial y}(\overline{v\theta}) + \overline{v^2}\frac{\partial}{\partial y}(\overline{u\theta})\right) \tag{9}$$

$$\overline{v^2\theta} = -2\tau'_u\overline{v^2}\frac{\partial}{\partial y}(\overline{v\theta}) \tag{10}$$

$$\overline{v\theta^2} = \tau'_u\overline{v^2}\frac{\partial}{\partial y}(\overline{\theta^2}), \tag{11}$$

with τ'_u defined as $\tau_u/c_{1\theta}$. A comparison between the measured triple moments and the above models is shown in Figs. 8–10. Uncertainties in the measured values of the LHSs of equations (9)–(11) are indicated on these figures. There is fair qualitative agreement in the cases of $\overline{uv\theta}$ and $\overline{v^2\theta}$ but the models change sign at larger values of η than the experimental data. Fackrell and Robins' [23] measurements in plumes downstream

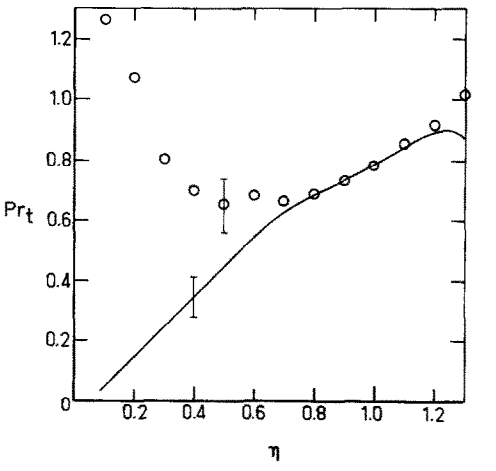

FIG. 7. Comparison of measured turbulent Prandtl number distribution with equation (8). ○, experiment; ——, equation (8), $c_{1\theta} = 2.26$.

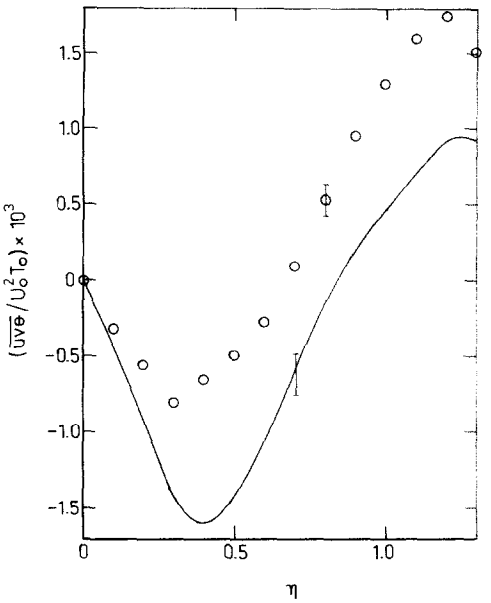

FIG. 8. Comparison of measured and modelled distributions of $\overline{uv\theta}$. ○, experiment; ——, experiment (9), $c_{1\theta} = 2.26$.

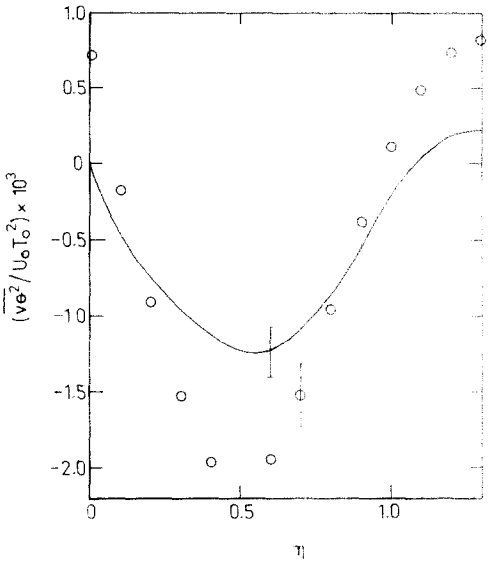

FIG. 10. Comparison of measured and modelled distributions of $\overline{v\theta^2}$. ○, experiment; ——, equation (11), $c_{1\theta} = 2.26$.

of point sources in a turbulent boundary layer also indicated qualitative agreement between measured and gradient-modelled distributions of $\overline{v^2\theta}$. In the case of $\overline{v\theta^2}$ (Fig. 10), the model generally underestimates the magnitude of the measured value although measured and modelled values change sign at about the same η. For comparison, Raupach and Legg [24] found that, downstream of an elevated line source in an equilibrium turbulent surface layer, equation (11) provided an adequate model for $\overline{v\theta^2}$ but neither equation (9) nor (10) was adequate.

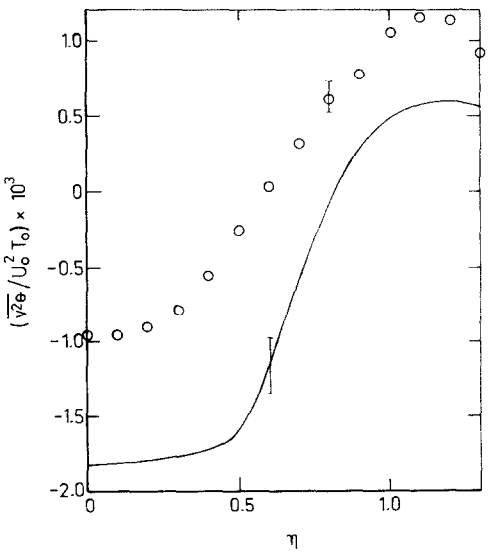

FIG. 9. Comparison of measured and modelled distributions of $\overline{v^2\theta}$. ○, experiment; ——, equation (10), $c_{1\theta} = 2.26$.

THE TIME SCALE RATIO R

For obvious reasons, in earlier second-order models, the temperature destruction was simply assumed to be given by

$$R = \frac{\tau_\theta}{\tau_u} = \text{constant}.$$

A value of 0.5 was suggested [21] for this constant on the basis of measurements in equilibrium thin shear flows. The same value was recommended by Pascal [25] for use in a plane jet into still air but no experimental data was given to support his recommendation. Spalding [26] chose a value of 0.56 for R to obtain agreement between his calculation of the variance $\overline{\theta^2}$ and measurements of this quantity in a round jet into still air. In view of the difference between the above values of R and its magnitude in the present flow (Fig. 3), it is pertinent to point out that this difference is consistent with, for example, the difference in turbulent Prandtl number between the present flow and a boundary layer for which a value of about 0.5 for R appears to be well established. With the assumption that production and destruction of $\overline{\theta^2}$ are approximately in balance (an assumption which is not violated in the present budget of $\overline{\theta^2}$ at a sufficient distance from the centreline [9]) it is easy to show that

$$R = \frac{a_1}{(a_\theta^2 Pr_t)}$$

where a_θ is the structural parameter $(\overline{v\theta}/\overline{\theta^2}^{1/2}\,\overline{uv}^{1/2})$ first introduced by Bradshaw and Ferriss [27]. Since the present values of a_1 ($\simeq 0.15$) and a_θ ($\simeq 0.55$), in the region $0.4 \leqslant \eta \leqslant 1.3$, do not differ appreciably from those reported in a boundary layer, the difference in the magnitude of R appears consistent with the smaller value of the turbulent Prandtl number ($\simeq 0.65$) in the

present flow (Browne and Antonia [15]) than in a boundary layer ($\simeq 0.90$). It should be noted that, for the determination of τ_θ, N was determined [9] from the sum of all three of its measured components whereas only the isotropic value of ε or $15\nu\overline{(\partial u/\partial x)^2}$, has been used in the determination of τ_u. As the measured value of N is larger (by about 50% at $\eta = 0$) than its isotropic value of $3\alpha\,\overline{(\partial\theta/\partial x)^2}$, the use of an isotropic value would have resulted in a corresponding larger value of R. It would, of course, be more appropriate to use the full (non-isotropic) estimate of ε in conjunction with the full value of N when R is evaluated. An appropriate non-isotropic estimate of ε could be inferred by difference from the budget of $\overline{q^2}$. This was not attempted since it would require the assumption of negligible pressure diffusion and, perhaps of secondary importance, the correlation $\overline{w^2v}$ was not measured. However, in the region where production and dissipation are approximately in balance for the $\overline{u\theta}$ and $\overline{v\theta}$ budgets, the isotropic value of ε was larger by about 10% than the production term $\overline{uv}\,\partial\bar{U}/\partial y$. This suggests that the present distribution of R (Fig. 3) would not be significantly changed if the isotropic estimate of ε were replaced by $\overline{uv}\,\partial\bar{U}/\partial y$.

CONCLUSIONS

The main contribution of this work may be summarised as follows:

(1) Measured budgets of longitudinal and lateral heat fluxes indicate that production and destruction terms are approximately equal away from the jet centreline. Although advection and diffusion terms are in balance, their magnitude is comparable, especially in the $\overline{v\theta}$ budget, to that of production or destruction.

(2) The same time scale yields adequate approximations for the pressure–temperature gradient correlations in either the $\overline{u\theta}$ or $\overline{v\theta}$ budgets, reflecting the near-equilibrium conditions for these budgets. The numerical value of the constant $c_{1\theta}$ is not significantly affected by whether a dynamic time scale, a scalar time scale or the geometric mean of these two time scales is used since the ratio of dynamic and scalar time scales is not very different from unity in this flow.

(3) Agreement between gradient-diffusion models and experimental distributions is, at best, only qualitative. It is unlikely that satisfactory quantitative agreement would be achieved by adjusting the numerical value of the time scale.

Acknowledgements—The author is grateful to Drs L. W. B. Browne and A. J. Chambers for their contributions to the experimental work. The assistance of Mr L. P. Chua with computations is also appreciated. The support of the Australian Research Grants Scheme is acknowledged.

REFERENCES

1. G. R. Newman, B. E. Launder and J. L. Lumley, Modelling the behaviour of homogeneous scalar turbulence, *J. Fluid Mech.* **111**, 217–232 (1981).
2. B. E. Launder and D. S. A. Samaraweera, Application of a second-moment turbulence closure to heat and mass transport in thin shear flows: I. Two-dimensional transport, *Int. J. Heat Mass Transfer* **22**, 1631–1643 (1979).
3. S. El Tahry, A. D. Gosman and B. E. Launder, The two- and three-dimensional dispersal of a passive scalar in a turbulent boundary layer, *Int. J. Heat Mass Transfer* **24**, 35–46 (1981).
4. W. P. Jones and P. Musonge, Modelling of scalar transport in homogeneous turbulent flows, *Proc. Fourth Symposium on Turbulent Shear Flows*, Vol. 17, pp. 18–24, Karlsruhe, (1983).
5. R. G. Owen, An analytical turbulent transport model applied to nonisothermal fully-developed duct flows. Ph.D. thesis, Pennsylvania State University (1973).
6. J. L. Lumley and T-H. Shih, Modeling Heat Flux in a Thermal Mixing Layer, *Proc. Int. Symposium on Refined Modelling of Flows*, Vol. 1, pp. 239–250, Paris (1982).
7. S. E. Elghobashi and B. E. Launder, Turbulent time scales and the dissipation rate of temperature variance in the thermal mixing layer, *Phys. Fluids* **26**, 2415–2419 (1983).
8. S. E. Elghobashi and J. C. LaRue, The effect of mechanical strain on the dissipation rate of a scalar variance, *Proc. Fourth Symposium on Turbulent Shear Flows*, Karlsruhe (1983).
9. R. A. Antonia, L. W. B. Browne, A. J. Chambers and S. Rajagopalan, Budget of the temperature variance in a turbulent plane jet, *Int. J. Heat Mass Transfer* **26**, 41–48 (1983).
10. R. A. Antonia and L. W. B. Browne, The destruction of temperature fluctuations in a turbulent plane jet, *J. Fluid Mech.* **134**, 67–83 (1983).
11. S. Corrsin, Remarks on turbulent heat transfer: an account of some features of the phenomenon in fully turbulent regions, *Proc. Thermodynamics Symposium*, Iowa (1953).
12. J. L. Lumley and B. Khajeh-Nouri, Computational modeling of turbulent transport, *Adv. Geophys.* **18A**, 169–192 (1974).
13. B. E. Launder, Heat and Mass Transport. In *Topics in Applied Physics*, Vol. 12, *Turbulence*, edited by P. Bradshaw, pp. 231–287. Springer-Verlag, Berlin (1976).
14. V. W. Goldschmidt, M. K. Moallemi and J. W. Oler, Structures and flow reversal in turbulent plane jets, *Phys. Fluids* **26**, 428–432 (1983).
15. L. W. B. Browne and R. A. Antonia, Measurements of turbulent Prandtl number in a plane jet, *J. Heat Transfer* **105**, 663–665 (1983).
16. R. A. Antonia and A. Prabhu, Reynolds shear stress and heat flux balance in a turbulent round jet, *AIAA Jl* **14**, 221–228 (1976).
17. J. C. Wyngaard, O. R. Coté and Y. Izumi, Local free convection, similarity, and the budgets of shear stress and heat flux, *J. Atmos. Sci.* **28**, 1171–1182 (1971).
18. E. F. Bradley, R. A. Antonia and A. J. Chambers, Streamwise heat flux budget in the atmospheric surface layer, *Boundary-Layer Meteorol.* **23**, 3–15 (1982).
19. A. S. Monin, On the symmetry properties of turbulence in the surface layer of air, *Izv. Atm. Ocean. Phys.* **1**, 45–54 (1965).
20. C. du P. Donaldson, R. D. Sullivan and H. Rosenbaum, A theoretical study of the generation of atmospheric-clear air turbulence, *AIAA Jl* **10**, 162–170 (1972).
21. C. Béguier, I. Dekeyser and B. E. Launder, Ratio of scalar and velocity dissipation time scales in shear flow turbulence, *Phys. Fluids* **21**, 297–310 (1978).
22. R. A. Antonia and H. Q. Danh, A local similarity model for the heat flux equation in a turbulent boundary layer, *Int. J. Heat Mass Transfer* **21**, 1002–1005 (1978).
23. J. E. Fackrell and A. G. Robins, Concentration fluctuations and fluxes in plumes from point sources in a turbulent boundary layer, *J. Fluid Mech.* **117**, 1–26 (1982).
24. M. R. Raupach and B. J. Legg, Turbulent dispersion from

an elevated line source: measurements of wind-concentration moments and budgets. *J. Fluid Mech.* **136,** 111–137 (1983).
25. A. Pascal, Contribution à l'étude d'un jet plan turbulent faiblement chauffé en écoulement incompressible. Thèse Docteur-Ingénieur, Institut National Polytechnique de Toulouse (1978).
26. D. B. Spalding, Concentration fluctuations in a round turbulent free jet, *Chem. Engng Sci.* **26,** 95–107 (1971).
27. P. Bradshaw and D. H. Ferriss, Calculation of boundary-layer development using the turbulent energy equation. IV. Heat transfer with small temperature differences, National Physical Laboratory Aero Report No. 1271 (1968).

SUR UN MODELE DE TRANSPORT DE CHALEUR POUR UN JET PLAN TURBULENT

Résumé—Des distributions de la corrélation température–gradient de pression sont obtenues à partir des bilans mesurés de flux de chaleur longitudinaux et latéraux dans la région d'auto-entretien d'un jet plan turbulent chauffé dans l'air au repos. Ces corrélations sont compatibles avec un modèle qui inclut seulement la contribution de l'interaction de turbulence aux fluctuations de pression. La comparaison entre le modèle et l'expérience n'est pas affectée par le choix de l'échelle de temps dans le modèle. Des termes dont les gradients forment la principale contribution à la diffusion dans les bilans pour les flux de chaleur et la variance de la température sont seulement qualitativement compatibles avec les modèles de type gradient.

MODELL DES WÄRMETRANSPORTS IN EINEM TURBULENTEN EBENEN STRAHL

Zusammenfassung—Die Verläufe der Temperatur–Druckgradient-Beziehungen ergaben sich aus der Messung der Beträge der längs- und quergerichteten Wärmestromdichten im selbsterhaltenden Bereich eines leicht beheizten, turbulenten, ebenen Strahls in ruhender Luft. Diese Beziehungen stimmen mit einem Modell überein, welches nur den Einfluß der turbulenten Wechselwirkung auf die Druckschwankungen berücksichtigt. Der Vergleich zwischen Rechenmodell und Experiment wird vom Zeitmaßstab des Modells nicht beeinflußt. Terme, deren Gradienten den Haupteinfluß auf die Diffusion (bei den Wärmestromdichten und Temperaturschwankungen) darstellen, stimmen nur qualitativ mit den Modellen vom Gradienten-Typus überein.

О МОДЕЛИ ТЕПЛОПЕРЕНОСА ДЛЯ ТУРБУЛЕНТНОЙ ПЛОСКОЙ СТРУИ

Аннотация—На основе измерений баланса продольного и поперечного турбулентных потоков тепла $u\theta$ и $v\theta$ в автомодельной области слабо нагретой плоской затопленной струи получена аппроксимация корреляции пульсации температуры–градиент пульсаций давления. Полученная аппроксимация соответствует моделям, учитывающим в рассматриваемой корреляции только 'возврат к изотропии'. Степень соответствия аппроксимации экспериментальным данным не зависит от выбора характерного временного масштаба. Что касается корреляций пульсаций давления с потоками тепла и пульсациями температуры, входящими в диффузионные члены, то предложенные аппроксимации лишь качественно соответствуют обычно используемым аппроксимациям градиентного типа.